Total-cross-section measurements for positron and electron scattering by O_2, CH_4, and SF_6

M. S. Dababneh
Department of Physics, Yarmouk University, Irbid, Jordan

Y.-F. Hsieh, W. E. Kauppila, C. K. Kwan, Steven J. Smith, T. S. Stein, and M. N. Uddin
Department of Physics and Astronomy, Wayne State University, Detroit, Michigan 48202
(Received 28 December 1987)

Total cross sections (Q_T's) have been measured for 1–500-eV positrons and electrons scattered by O_2, CH_4, and SF_6 using a beam-transmission technique. The positron Q_T's are compared with the corresponding electron Q_T's for each target gas. It is found that the positron Q_T's are, in general, lower than the electron results. There are no prominent structures observed for positron scattering at low energies that would be comparable to the narrow shape resonances observed for electrons scattering from various molecules, such as SF_6. The positron Q_T curve for CH_4 reveals a significant increase in the vicinity of its positronium formation threshold, while the O_2 and SF_6 curves are monotonically increasing in this vicinity. At the highest energies investigated, there are indications of a tendency toward merging of the positron and electron Q_T's for these gases. Interesting similarities are found in a comparison of the present positron and electron Q_T curves for CH_4 with prior comparison measurements for argon.

I. INTRODUCTION

This paper is part of a continuing study[1] which aims to measure the total cross sections (Q_T's) of positrons and electrons scattered by room-temperature gases. Total-cross-section measurements for electrons scattering from molecules are of importance in a variety of applications, such as gaseous electronics (e.g., discharges and dielectrics), plasma physics, and investigations of planetary atmospheres. Measurements of Q_T's for positrons and electrons scattered by the same molecules, when compared with each other and with theoretical calculations, may also help lead to a better understanding of the fundamental interaction mechanisms contributing to electron scattering. This approach has been adopted by our group where positron and electron Q_T's are measured in the same apparatus under nearly identical conditions, and meaningful comparisons of the scattering for these particles can be made. Although positrons and electrons differ only by the sign of their electric charge, there are interesting differences in their interaction with atoms and molecules. The static and polarization potentials are both attractive for electrons, while for positrons the static interaction changes sign so as to result in an overall weaker interaction for positrons than for electrons. There is also no exchange interaction for positrons as there is for electrons. An inelastic channel that is only open for positrons is that of positronium formation. At sufficiently high energies the static interaction becomes the only significant interaction for both projectiles, with the result being that the corresponding positron and electron Q_T's eventually will be expected to merge. There are other, more subtle, differences between the scattering of positrons and electrons by molecules.[2] For example, it is not clear whether there are effects which would produce resonances in positron scattering, although shape resonances are prominent in many low-energy electron Q_T's and are understood to be due to the formation of virtual negative ions. In this paper we present measurements of Q_T's for positrons and electrons scattered by O_2, CH_4, and SF_6. The projectile energy range is 1–500 eV, except for the e^--O_2 system, where a different electron source was used and the lower-energy limit was 5 eV. It is to be noted that preliminary reports of this work have been made elsewhere.[3]

II. EXPERIMENTAL METHOD

The experimental apparatus, procedure and error analysis have been described in detail elsewhere.[4,5] Briefly, a monochromatic beam of slow positrons (energy width <0.1 eV) is extracted from an ^{11}C source, which is produced by bombarding an ^{11}B target with a 4.75-MeV proton beam from a Van de Graaff accelerator. Total cross sections are deduced from the expression

$$I = I_0 e^{-nLQ_T}, \tag{1}$$

where I_0 is the detected beam intensity without gas in the scattering region, I is the detected beam intensity with gas of number density n in the scattering region, and L is the beam path length through the scattering region. For electron work, a thermionic electron source (Philips cathode) replaces the positron source. Since it was found that small amounts of molecular oxygen in the source chamber enhance the electron emission of the Philips cathode, a heated tungsten wire was used as the electron source for the e^--O_2 measurements, and the source chamber was maintained at a constant pressure of O_2, regardless of whether gas was or was not in the scattering region, which enabled the tungsten filament to produce a stable primary beam intensity. The lowest electron ener-

gy attained using this modified electron source was 5.1 eV with an energy width of about 0.15 eV, which was comparable to the electron energy width obtained with the Philips cathode. The energies of the projectile beams were determined by the voltage applied to the source, and the absolute energies were established using the retarding potential technique.[5] This technique was also checked by observing the cross-section resonance at 19.3 eV for electrons colliding with helium. In the 5–30 eV energy range, in which we observed resonances for the e^--SF_6 total cross sections, we estimate that the uncertainty associated with our assigned projectile energies was ±0.2 eV.

The estimated errors in the present Q_T measurements, determined in the same manner as described earlier,[4] are listed in Table I with the "experimental errors" representing the combining in quadrature of statistical errors and the estimated errors associated with measurements of the projectile beam currents, the target-gas number density, and the projectile path length through the scattering region, while the "maximum errors" result from a simple addition of each individual error component. It is to be noted that the errors for the positron and electron comparison Q_T measurements are smaller than those for the absolute Q_T measurements for the same target gas because several of the individual error components equally affect the positron and electron measurements. In addition, a standard procedure in every data run is to measure the Q_T's with different target-gas densities to ensure that the results are not pressure dependent, as is shown in Fig. 1.

It should be noted that the error estimates discussed above do not include a potential source of error arising from the incomplete discrimination of projectiles scattered at small forward angles, which would result in the measured Q_T values being lower than the actual values. Independently, a retarding element and a small exit aperture from the scattering region provide for discrimination against small-angle scattering. The retarding element is effective in discriminating against projectiles which have suffered an energy loss of more than a few tenths of an eV. As a result, the discrimination against electronic excitation, ionization, and positronium formation should be complete, while the discrimination against rotational and vibrational excitation, and elastic scattering may be incomplete. Following the method of analysis used earlier,[4] the estimated discrimination angles for the present measurements for elastic scattering have been determined and are listed in Table II. The smaller of the two angles listed for each energy represents the upper limit on the estimated angular discrimination. With the estimated discrimination angles given in Table II and detailed elastic differential cross sections, where available, it would be possible to estimate the magnitude of the errors in the measured Q_T values due to this effect if there were no inelastic scattering present. In the case of rotational and vibrational excitation the angular discrimination would be better than that for elastic scattering due to the small, but finite, inelastic energy loss and the effect of the retarding element.

TABLE I. Estimated percentage errors for the present absolute and $e^{+,-}$ comparison total-cross-section measurements. The "experimental errors" are shown outside the parentheses while the "maximum errors" are enclosed by parentheses. Note that the estimated errors do not include the errors associated with incomplete discrimination against small forward angle scattering.

	Absolute measurements		Comparison measurements	
	e^+	e^-	e^+	e^-
Statistical	2(2)	1(1)	2(2)	1(1)
I,I_0	3(4)	2(3)	3(4)	2(3.5)
L	2(3)	1(2)	1(1)	0.2(0.5)
n	4(7)	4(7)	0(0)	0(0)
Total	6(16)	5(13)	4(7)	3(5)

III. RESULTS AND DISCUSSION

The present measured total cross sections and associated statistical uncertainties are listed in Table III.

A. Molecular oxygen

The present Q_T results for low- and intermediate-energy positrons scattered by molecular oxygen are shown in Figs. 2 and 3, respectively, along with prior measurements.[6–8] The present data indicate a Q_T curve that increases smoothly from the lowest energy through the positronium formation threshold (5.3 eV), with no significant change in slope, to a broad maximum at

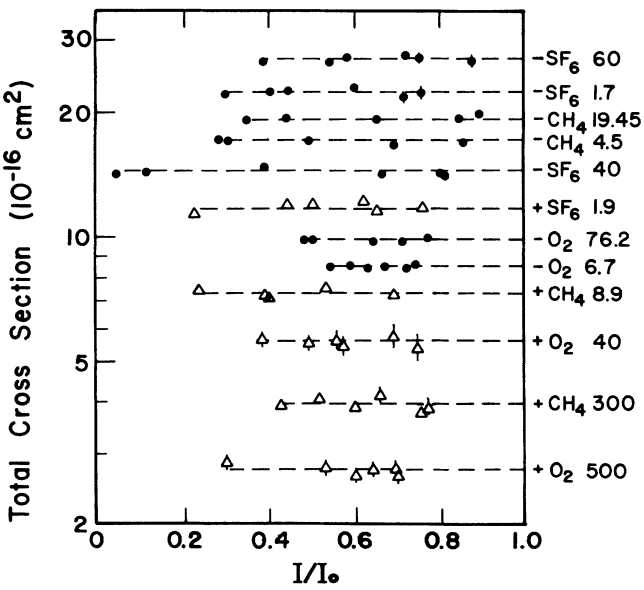

FIG. 1. Measured total cross sections vs attenuation ratios I/I_0 for various projectile-target combinations. The right-hand column indicates the projectile (" + " for positrons and " − " for electrons), target gas, and projectile energy in eV. The bars represent one standard deviation of the measured cross sections except when they are encompassed by the dots or triangles.

TABLE II. Estimated discrimination angles in degrees calculated for the retarding potential procedure and for effects due to exit aperture size. The labeling for the retarding potential effect is R and for the exit aperture size is indicated by A.

	O_2		CH_4		SF_6	
	e^+	e^-	e^+	e^-	e^+	e^-
E (eV)	A,R	A,R	A,R	A,R	A,R	A,R
5	21,31	5,28	18,35	5,8	21,22	6,13
10	30,26	4,16	17,21	5,10	17,23	5,9
20	16,23	5,10	16,18	5,8	18,20	5,8
50	15,19	4,5	17,16	5,5	18,15	3,6
100	18,9	4,7	13,10	4,4	17,13	5,5
300	7,11	6,6	15,11	5,6	13,7	5,4
500	8,14	6,3	8,11	4,4	8,14	5,5

around 30 eV. This behavior is quite unique because it is the first room-temperature gas studied in this laboratory for which the total cross section does not have an appreciable change in slope in the vicinity of the positronium formation threshold. Also, because of our lower-energy limit (0.75 eV), it was not possible to observe if there is an indication of a sharp increase in the cross section toward lowest energies, as has been observed for all other gases studied in this laboratory.[1(b)] In general, the present e^+-O_2 results are in fair agreement with those of Charlton *et al.*[8] in the 2–20 eV region and with Charlton *et al.*[7] in the 20–500 eV range. However, the results of Charlton *et al.*[7] are consistently higher than our results for energies below 100 eV and consistently lower for energies above 200 eV. This is noteworthy, since this systematical discrepancy is not limited to the present e^+-O_2 measurements (see below). Charlton *et al.*[8] also found statistically significant structures in their Q_T measurements between 8 and 13 eV, which they thought may be due to electronic excitation or possibly e^+-O_2 compound state formation. The present experiment is unable to confirm this feature, although it might be found within the statistical uncertainties. Due to the lack of pertinent information on the elastic differential cross sections for e^+-O_2, no error estimate can be made on our e^+-O_2 Q_T data associated with the effects of finite angular discrimination of the apparatus.

The present intermediate- and low-energy measurements of e^--O_2 total scattering cross sections are shown in Figs. 3 and 4, respectively, together with other measurements.[9–15] Comparing our low-energy results (Fig. 4) with other measurements, the present e^--O_2 results agree fairly well with those of Sunshine *et al.*[11] and Zecca *et al.*[15] below 10 eV, while they are, respectively, 20% and 10% lower than our results above 12 eV. Our results agree well in the shape of the curve with those of Griffith *et al.*,[9] with their results being about 12% lower than the present measurements over all energies of overlap. The elastic cross sections of Shyn and Sharp[13] are higher below 10 eV and lower above 10 eV than our results. The present results are about 20% higher than those of Bruche[10] and Salop and Nakano[12] above 12 eV due to a noticeable decrease in their measured cross sections at this energy. In the intermediate-energy range (Fig. 3), the e^--O_2 total cross sections display a smoothly declining curve. Between 20 and 100 eV, our results are appreciably higher than the measurements of Sunshine *et al.*[11] and are, in general, higher than the results of Zecca *et al.*,[15] except at 100 eV where they agree well with our results. Above 100 eV, the present measurements agree remarkably well with those of Dalba *et al.*[14] For the sake of clarity in Fig. 3, the intermediate-energy elastic integral cross-section measurements of Shyn and Sharp[13] and calculations of Wedde and Strand[16] and Khare and Raj[17] are not shown, with their respective results at intermediate energies for elastic integral cross sections being about 20% lower than the present measurements. Also in Fig. 3, the e^--O_2 and e^+-O_2 total cross sections are compared. For all the energies studied, the electron Q_T values are higher than the positron results, with both curves exhibiting maxima in the 20–30 eV region, and the two cross-section curves approaching each other at the highest energies. At 500 eV, the e^--O_2 Q_T is still 25% higher than the e^+-O_2 Q_T.

To estimate the amount by which the present e^--O_2 Q_T results may be low due to incomplete discrimination against small-angle scattering, the elastic angular distribution measurements of Shyn and Sharp,[13] and Bromberg,[18] and the calculated differential cross sections of Khare and Raj[17] along with the estimated discrimination angles in Table II are used. The estimated errors due to this effect for electron energies of 15 and 500 eV are 2% and 3%, respectively.

B. Methane

Much attention has been devoted in the last few years to the scattering of positrons and electrons by methane, since this molecule has been found to be an important component in the atmosphere of some of the outer planets and their satellites.

The present e^+-CH_4 Q_T results are shown in Figs. 5 and 6 along with prior measurements of Charlton *et al.*,[7,8] Floeder *et al.*,[19] and Sueoka and Mori,[20] and the recent calculations of Jain.[21] The present results show a substantial increase in the cross section below 2 eV and at the positronium formation threshold (6.2 eV) with a minimum occurring at about 5 eV. A maximum is

TABLE III. Results of measured total cross sections and statistical uncertainties (in units of 10^{-16} cm^2) for $e^{+,-}$-O_2, CH_4, and SF_6

E (eV)	Q_T (e^+-O_2)	E (eV)	Q_T (e^--O_2)	E (eV)	Q_T (e^+-CH_4)
0.75	1.5 ±0.05	5.2	8.6±0.15	1.0	8.1±0.5
1.0	1.9 ±0.07	6.7	8.8±0.1	1.42	6.8±0.3
1.4	1.9 ±0.15	9.3	10.8±0.1	1.92	5.3±0.4
1.9	2.0 ±0.1	10.5	10.8±0.1	2.7	5.4±0.2
2.8	2.4 ±0.1	11.7	11.8±0.2	3.4	5.1±0.3
3.5	2.7 ±0.1	13.1	12.1±0.2	3.8	4.8±0.2
4.5	3.0 ±0.1	14.2	11.7±0.2	4.3	4.8±0.2
4.9	3.0 ±0.1	15.3	11.6±0.2	4.9	4.6±0.2
5.4	3.1 ±0.15	16.5	11.9±0.2	5.2	4.9±0.2
5.9	3.6 ±0.1	18.1	11.9±0.1	5.6	5.1±0.2
6.5	3.8 ±0.15	19.0	11.9±0.3	5.9	4.7±0.2
6.8	3.9 ±0.1	20.1	12.2±0.1	6.6	5.4±0.2
7.2	4.0 ±0.1	21.5	11.7±0.1	7.1	5.4±0.2
7.9	4.2 ±0.1	23.0	12.3±0.1	7.8	6.7±0.2
8.2	4.4 ±0.1	23.8	11.8±0.1	8.9	7.5±0.2
8.9	4.7 ±0.1	24.8	12.2±0.2	9.8	8.3±0.2
9.4	4.6 ±0.1	26.3	12.5±0.1	11.0	8.7±0.3
9.9	4.8 ±0.1	28.0	11.8±0.2	12.0	9.1±0.4
10.4	4.9 ±0.1	28.8	12.2±0.1	13.3	9.5±0.3
10.9	5.0 ±0.1	30.4	11.8±0.1	14.2	9.5±0.3
11.4	5.2 ±0.1	31.3	12.0±0.1	15.2	9.6±0.2
12.0	5.5 ±0.15	33.2	12.0±0.3	16.1	9.7±0.2
12.4	5.3 ±0.1	35.0	12.1±0.2	17.6	9.7±0.3
12.8	5.5 ±0.15	36.4	12.2±0.2	18.0	10.1±0.3
13.5	5.6 ±0.1	38.4	12.0±0.3	20.1	10.1±0.3
14.0	5.2 ±0.15	40.2	11.7±0.2	22.0	10.1±0.2
15.0	5.7 ±0.15	43.0	11.7±0.2	23.5	10.5±0.2
16.1	5.8 ±0.15	45.5	11.2±0.2	24.5	10.5±0.2
16.9	5.9 ±0.1	46.4	11.5±0.2	25.4	10.7±0.2
18.4	6.2 ±0.1	47.7	10.7±0.1	26.6	10.9±0.2
19.0	6.0 ±0.2	48.9	11.5±0.2	27.3	10.3±0.3
21.2	6.3 ±0.1	51.1	12.1±0.3	29.4	10.5±0.2
21.9	6.2 ±0.15	55.0	10.7±0.2	30	10.6±0.2
22.6	6.6 ±0.2	60.7	11.1±0.2	40	10.1±0.2
24.1	6.7 ±0.2	65.7	10.3±0.4	50	9.8±0.2
25.1	6.5 ±0.1	69.8	10.7±0.1	60	9.4±0.1
28.3	6.8 ±0.2	72.4	10.2±0.1	75	8.6±0.1
30.2	6.6 ±0.1	76.2	9.9±0.1	100	7.7±0.1
40.1	6.4 ±0.1	81.0	9.2±0.2	150	6.3±0.1
50.1	6.5 ±0.1	87.9	9.3±0.15	200	5.4±0.1
60.4	6.3 ±0.1	92.7	9.0±0.1	300	4.0±0.1
70.1	6.3 ±0.1	96.1	8.9±0.1	400	3.4±0.2
80.3	6.1 ±0.1	102.7	9.0±0.1	450	3.0±0.1
90.3	5.8 ±0.1	113	8.3±0.1	500	2.6±0.2
100	5.5 ±0.1	127	8.0±0.1		
150	4.8 ±0.1	153	7.2±0.1		
200	4.5 ±0.1	200	6.5±0.1		
300	3.66±0.05	300	4.9±0.1		
400	3.18±0.07	400	4.3±0.1		
500	2.78±0.05	500	3.5±0.1		
600	2.49±0.04				

E (eV)	Q_T (e^--CH_4)	E (eV)	Q_T (e^+-SF_6)	E (eV)	Q_T (e^--SF_6)
1.44	3.9±0.1	1.0	14.2±0.3	0.98	22.9±0.3
1.8	5.3±0.1	1.4	11.6±0.3	1.4	22.4±0.2
2.6	8.3±0.1	1.9	11.5±0.4	1.44	23.3±0.15
3.5	12.5±0.2	2.4	10.8±0.4	1.9	23.5±0.2
4.1	14.3±0.2	3.2	11.1±0.3	2.3	24.1±0.2

TABLE III. (*Continued*).

E (eV)	Q_T (e^--CH_4)	E (eV)	Q_T (e^+-SF_6)	E (eV)	Q_T (e^--SF_6)
4.5	17.2±0.1	4.2	11.1±0.2	2.8	23.7±0.1
4.9	18.4±0.2	4.9	10.7±0.2	3.7	22.9±0.2
5.7	23.0±0.3	5.5	10.6±0.15	4.2	22.3±0.2
6.4	25.3±0.3	6.2	11.1±0.2	4.7	23.2±0.5
7.8	28.1±0.2	7.1	10.9±0.2	5.1	24.1±0.2
8.1	28.4±0.5	8.0	11.4±0.1	5.7	27.7±0.2
9.8	27.2±0.2	9.1	11.4±0.3	6.2	28.1±0.3
11.9	25.3±0.2	10.2	11.7±0.2	6.7	31.5±0.5
14.6	23.9±0.2	11.0	11.9±0.3	7.3	29.7±0.4
19.45	19.5±0.3	11.7	12.4±0.2	7.5	29.9±0.3
24.5	17.6±0.2	13.0	13.0±0.3	7.7	29.9±0.3
29.25	16.2±0.2	14.2	13.4±0.1	8.7	28.0±0.15
34.7	15.2±0.2	15.0	13.4±0.3	9.7	27.1±0.2
39.3	14.5±0.2	16.1	13.8±0.2	10.7	28.0±0.2
44.7	13.6±0.2	18.3	14.3±0.2	11.2	30.8±0.2
49.6	12.7±0.2	20.2	14.3±0.3	11.7	32.8±0.2
100	9.1±0.2	21.9	14.9±0.2	11.9	33.5±0.2
200	6.2±0.1	24.8	14.9±0.2	12.1	32.1±0.3
300	4.6±0.1	29.9	14.9±0.2	12.7	28.5±0.1
400	3.7±0.1	40.1	15.0±0.2	13.2	26.7±0.2
500	3.1±0.1	49.8	14.8±0.2	14.5	26.2±0.2
		75	14.7±0.2	16.5	25.9±0.1
		100	13.9±0.2	19.6	26.9±0.1
		150	12.7±0.3	24.6	29.0±0.2
		200	12.2±0.2	27.2	28.1±0.3
		300	10.5±0.2	30.0	29.1±0.3
		400	8.7±0.3	39.8	28.4±0.2
		450	8.5±0.1	41.6	28.8±0.2
		500	7.8±0.1	45.7	28.9±0.2
				49.6	28.4±0.3
				54.8	28.9±0.2
				56.5	29.0±0.2
				59.6	28.0±0.3
				67.5	27.0±0.4
				74.5	26.0±0.3
				79.6	25.8±0.3
				84.7	25.2±0.3
				89.4	24.4±0.3
				94.7	25.4±0.3
				99.2	24.3±0.3
				125	22.7±0.3
				150	20.6±0.3
				175	19.1±0.2
				200	18.2±0.1
				250	16.4±0.1
				300	14.6±0.1
				400	13.5±0.1
				500	11.6±0.1

observed in Q_T at about 25 eV and a steady decrease toward higher energies. Our results are in good agreement with those of Sueoka and Mori. The present results vary between being higher, lower, and in good agreement with the measurements of Charlton *et al.* and the calculations of Jain at various energies of overlap. The measurements by Floeder *et al.* are higher than the present measurements below 20 eV and in good agreement above 20 eV.

Figure 7 shows our measurements of low-energy e^--CH_4 Q_T's along with prior measurements[10,19,20,22–25] and theoretical calculations.[26,27] We should indicate that, for the sake of clarity, below 2 eV we only present the recent measurements of Lohman and Buckman,[25] which show a Ramsauer minimum at about 0.4 eV. Their results are in good agreement with the pioneering measurements of Ramsauer and Kollath.[28] Our results show a steady increase of Q_T with increasing energy where it peaks at about 8 eV, and then start decreasing with increasing energy. Below 6 eV, our results are in good agreement with the measurements of Sueoka and Mori,[20] Jones,[24] and Lohman and Buckman.[25] From 6 to 20 eV our results are higher than all others shown, but are closest to the same prior measurements,[20,24,25] and the calculations of Jain.[27]

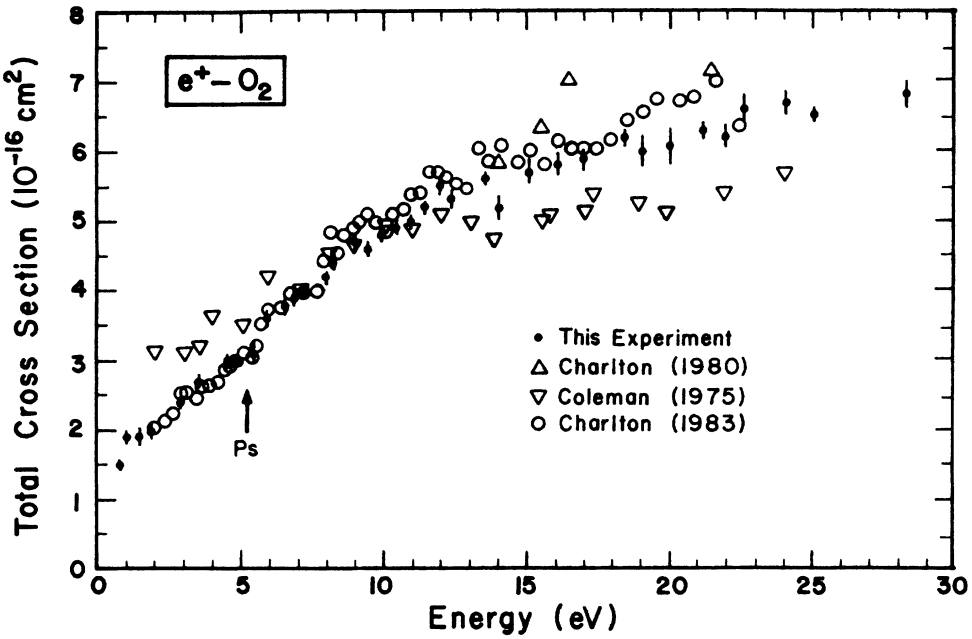

FIG. 2. Low-energy e^+-O_2 total cross sections. The present results are shown along with the measurements of Charlton *et al.* (Ref. 7), Charlton *et al.* (Ref. 8), and Coleman *et al.* (Ref. 6). The positronium formation threshold is indicated by the arrow.

Intermediate-energy $e^- + CH_4$ Q_T results are presented in Fig. 8 along with other measurements[19,20,29] and a calculation.[27] The results show a continuous decrease in the cross section with increasing energy. Although our results are in fair agreement in the shape of the curve with the other Q_T measurements[19,20] and the calculation,[27] the general trend is that our results are 2–20 % higher than their results at all energies except for the calculations of Jain[27] above 200 eV where his results are slightly ($< 10\%$) higher than the present results. The results obtained from the elastic and excitation differential cross-section measurements of Vuskovic and Trajmar[29] average 25% lower than our results.

Both $e^- + CH_4$ and $e^+ + CH_4$ Q_T's are shown in Fig. 9 for the purpose of comparison. The positron Q_T's are everywhere lower than the electron results except at very low energies. The positron curve peaks at a higher energy (about 25 eV) than is found for electrons (about 8 eV). The cross section then starts decreasing with increasing energy, with a sharper decrease observed for electrons where the difference in the electron and positron cross sections gets smaller and becomes less than 15% above 100 eV.

Estimates of the amount of error due to the finite angular discrimination of our apparatus are made using the discrimination angles listed in Table II together with the theoretical differential elastic cross sections of Jain[27,30] and the rotationally summed elastic differential cross sections of Abusalbi *et al.*[31] For the e^+-CH_4 Q_T's, we estimate that our present results at 25 and 500 eV may be low by 1% and 12%, respectively, and for e^--CH_4 Q_T's at 10 and 500 eV, the respective errors amount to 2% and 5%.

Another interesting aspect regarding the scattering of positrons and electrons by methane is its similarity with argon. Methane has a high degree of symmetry with a

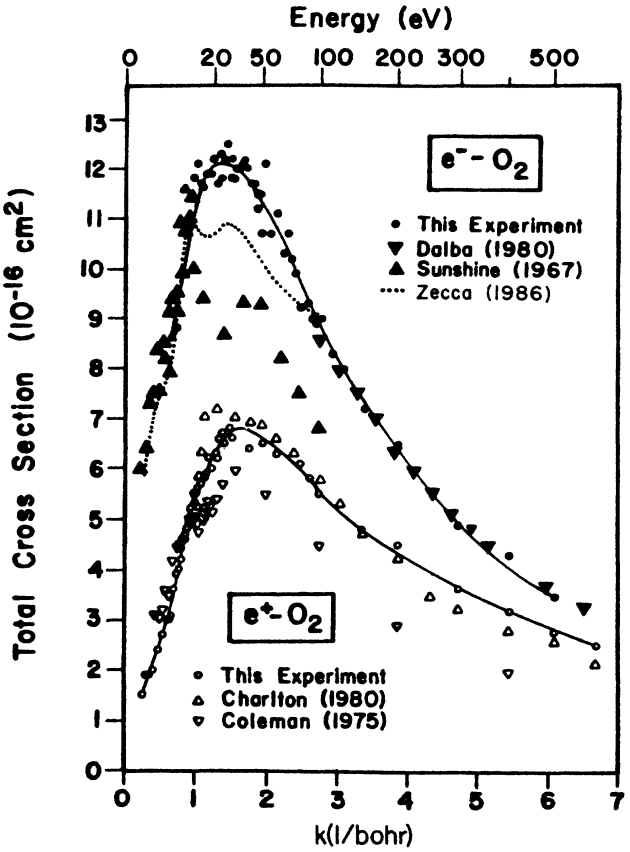

FIG. 3. Comparison of e^+- and e^--O_2 total cross sections up to intermediate energies. The positron data are shown along with the measurements of Charlton *et al.* (Ref. 7) and Coleman *et al.* (Ref. 6). The present electron measurements are shown along with the measurements of Sunshine *et al.* (Ref. 11), Dalba *et al.* (Ref. 14), and Zecca *et al.* (Ref. 15). The solid curves are intended to guide the eye through the present measurements.

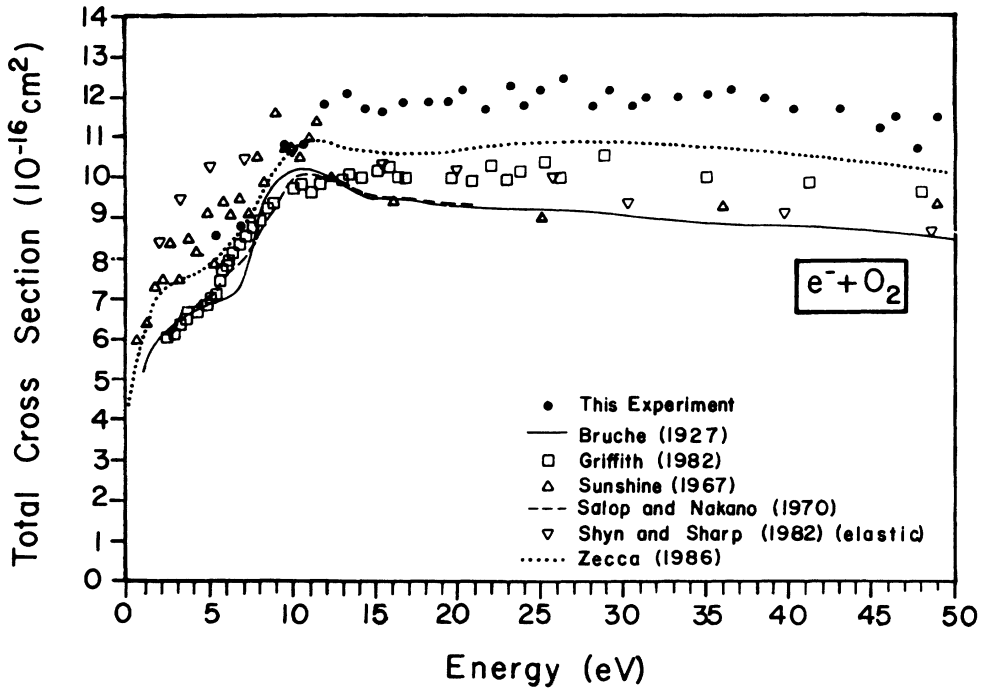

FIG. 4. Low-energy e^--O_2 total cross sections. The present results are shown along with the measurements of Bruche (Ref. 10), Sunshine *et al.* (Ref. 11), Salop and Nakano (Ref. 12), Shyn and Sharp (Ref. 13), Griffith *et al.* (Ref. 9), and Zecca *et al.* (Ref. 15).

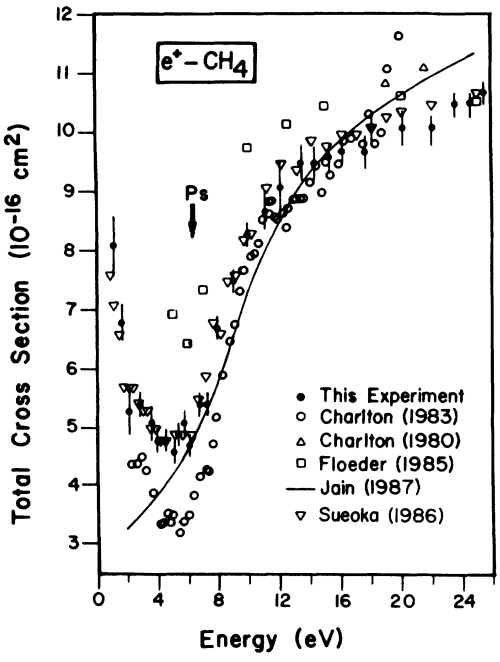

FIG. 5. Low-energy e^+-CH_4 total cross sections. The present results are shown along with the measurements of Charlton *et al.* (Refs. 7 and 8), Sueoka and Mori (Ref. 20), and Floeder *et al.* (Ref. 19), and the calculated results of Jain (Ref. 21). The arrow indicates the positronium formation threshold.

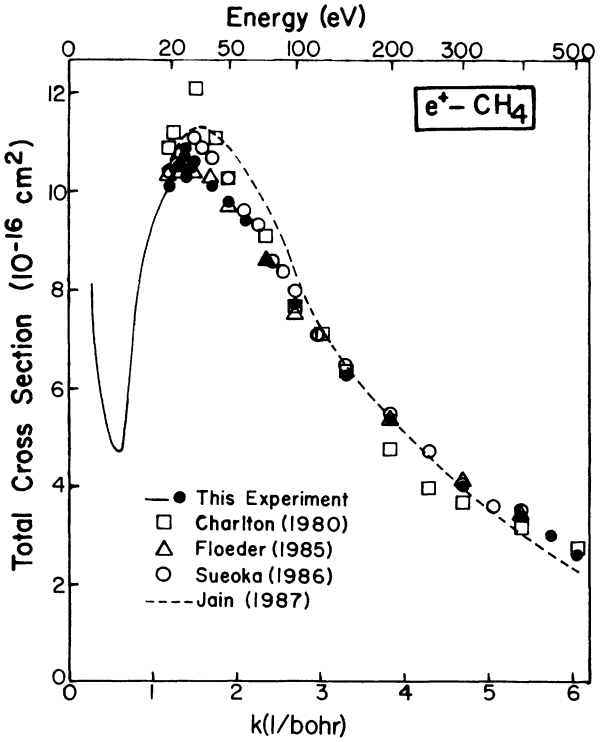

FIG. 6. Intermediate-energy e^+-CH_4 total cross sections. The present results are shown along with the measurements of Charlton *et al.* (Ref. 7), Floeder *et al.* (Ref. 19), Sueoka and Mori (Ref. 20), and the recent calculation of Jain (Ref. 21).

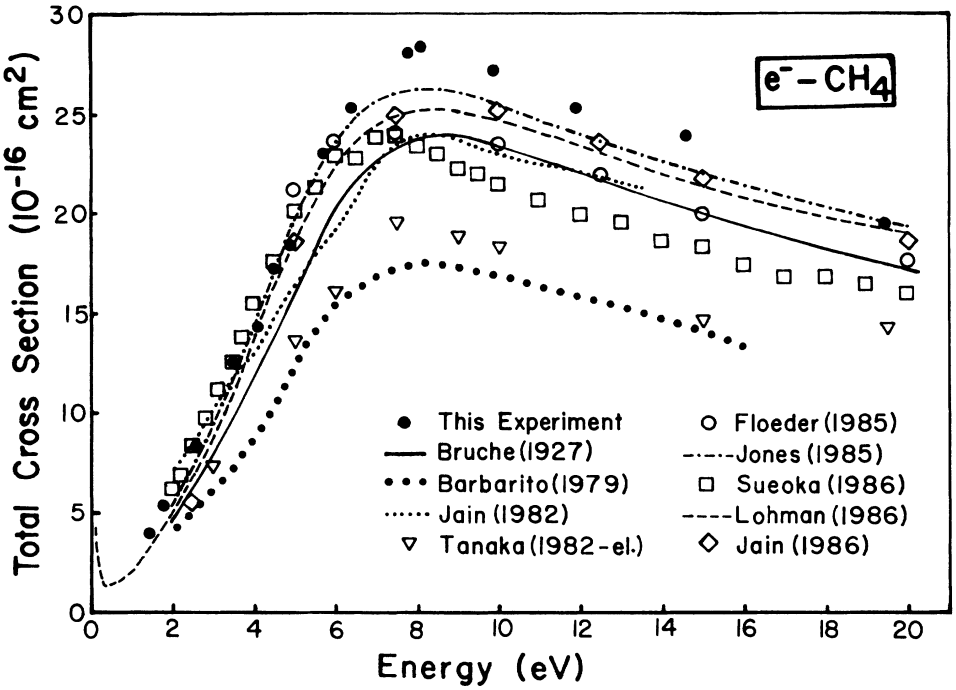

FIG. 7. Low-energy e^--CH_4 total cross sections. The present results are shown with the measurements of Bruche (Ref. 10), Barbarito *et al.* (Ref. 22), Tanaka *et al.* (Ref. 23), Floeder *et al.* (Ref. 19), Jones (Ref. 24), Sueoka and Mori (Ref. 20), and Lohman and Buckman (Ref. 25), and the calculations of Jain and Thompson (Ref. 26) and Jain (Ref. 27).

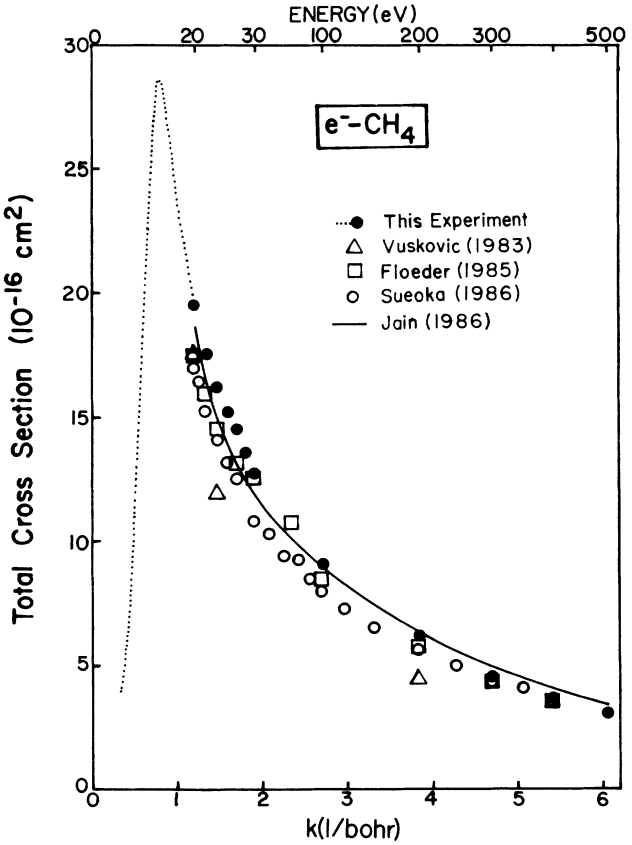

FIG. 8. Intermediate-energy e^--CH_4 total cross sections. The present results are shown along with the measurements of Floeder *et al.* (Ref. 19), Sueoka and Mori (Ref. 20), and Vuskovic and Trajmar (elastic and excitation, Ref. 29), and the theoretical calculations of Jain (Ref. 27).

closed-shell structure, and zero permanent dipole and quadrupole moments. Massey *et al.*[32] have commented that, taking into account the highly symmetric average field in which the electrons move in methane, close similarities in the behavior to argon would be expected for electrons less than 20 eV. More recently, Tanaka *et al.*[23] have found interesting similarities in the shape and magnitude of the elastic differential cross sections of $e^- + CH_4$ and $e^- + Ar$ at energies ≤ 10 eV. It is therefore not surprising to find similarities in the e^--CH_4 and e^--Ar total cross sections. Indeed, comparing Figs. 7 and 9 with Fig. 2 of Ref. 33 and Fig. 5 of Ref. 4, we find that both the e^--CH_4 and e^--Ar Q_T curves have unusually low Ramsauer-Townsend minima below 1 eV and rise rapidly toward higher energies, forming broad maxima at 8 and 13 eV for CH_4 and Ar, respectively. The minima at low energies are so low that the e^- Q_T's fall well below the corresponding e^+ Q_T's at these energies for both gases. The same situation prevails in the comparison of the e^+ Q_T's (Figs. 5 and 9 versus Fig. 3 of Ref. 33 and Fig. 5 of Ref. 4). Except for the shallow Ramsauer-Townsend minimum for Ar, both curves rise rapidly toward lower energies, have broad minima below the respective positronium formation thresholds, and increase rapidly above these thresholds, eventually reaching a peak at about 25 eV for CH_4 and 40 eV for Ar.

C. Sulfur hexafluoride

There is a considerable amount of experimental and theoretical work in the literature on the e^--SF_6 system, including photoionization cross sections, x-ray absorption, emission, and electron scattering measurements. Of special interest is electron attachment in SF_6 due to its

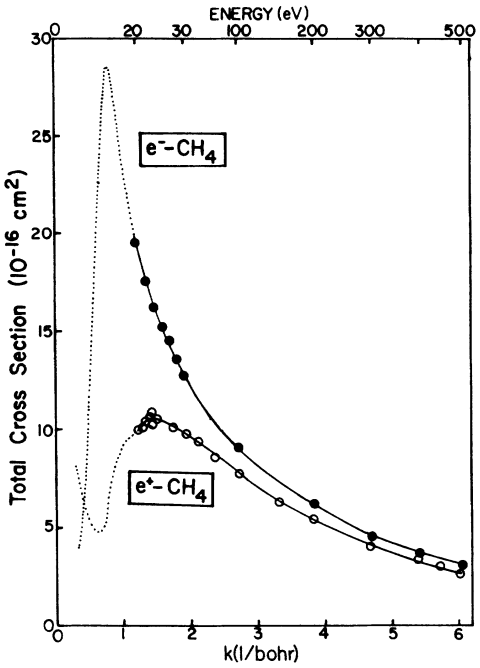

FIG. 9. Comparison of the present e^+- and e^--CH_4 total-cross-section measurements. The dotted curves represent our lower-energy results, while the solid line is drawn through our higher-energy results.

ability to attach electrons at very low energies.[34] This property is the physical basis for the application of SF_6 as a gas dielectric. The situation is quite different for the scattering of positrons by SF_6. There is no experimental or theoretical work presently known for this system.

The present low- and intermediate-energy e^+-SF_6 Q_T results are shown in Figs. 10 and 11, respectively. The total cross sections increase rapidly below 2 eV toward lower energies and above 7 eV toward higher energies with a broad minimum at about 5 eV. While it is reasonable to attribute the rise of the Q_T's between 6 and 20 eV to inelastic scattering, our data do not seem to show an abrupt increase at the positronium formation threshold

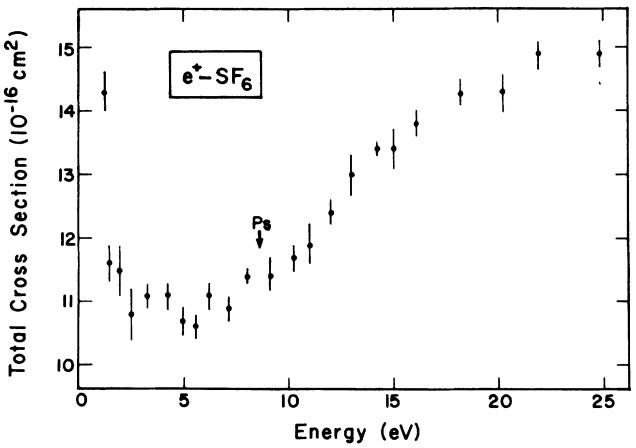

FIG. 10. Low-energy e^+-SF_6 total cross sections. The positronium formation threshold is indicated by the arrow.

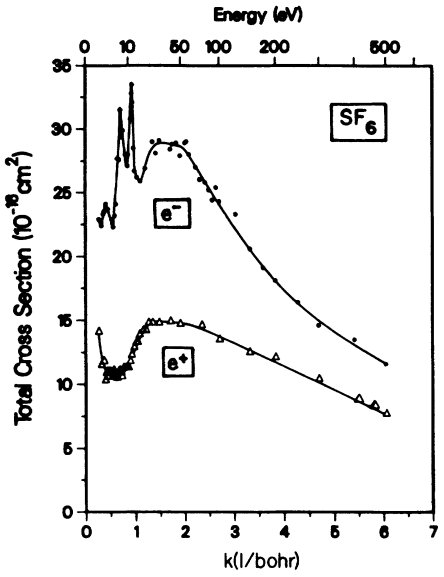

FIG. 11. Comparison of e^+- and e^--SF_6 total cross sections up to intermediate energies. A solid line is drawn through the experimental points.

(8.4 eV), indicating that other inelastic processes (e.g., target excitation) may contribute to the Q_T increases at these energies. The total cross sections reach a maximum at around 25 eV and decline steadily toward higher energies (Fig. 11).

Contrary to the rather smooth Q_T curve for e^+-SF_6, the Q_T's for electrons scattered by the same gas show a series of very distinct resonance peaks in the 1–30 eV energy range. This is shown in Figs. 11 and 12 along with the measurements of Kennerly *et al.*,[35] Rohr,[36] Ferch *et al.*,[37] and the theoretical work of Dehmer *et al.*[38] The present measurements find resonances at 2.3, 6.7, and 11.9 eV with cross sections of 24.1±0.2, 31.5±0.5, and 33.5±0.2 Å^2, respectively. These correspond to the a_{1g}, t_{1g}, and t_{2g} orbital assignments of Dehmer *et al.*

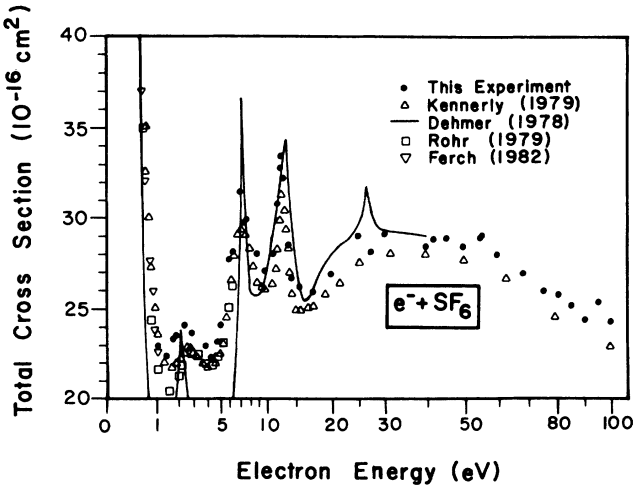

FIG. 12. Low-energy e^--SF_6 total cross sections. The present results are shown along with the measurements of Kennerly *et al.* (Ref. 35), Rohr (Ref. 36), and Ferch *et al.* (Ref. 37), and the theoretical results of Dehmer *et al.* (Ref. 38).

There is good agreement with the results of Kennerly *et al.* in regards to the energies of these resonances, but the present results are approximately 7% higher at the peaks. We note also that the experimental results of the lower-energy resonances (a_{1g},t_{1g}) show substantially broader peaks than the sharp and strong resonances predicted by Dehmer *et al.* In addition, both Kennerly *et al.* and this experiment fail to show the e_g resonance predicted by Dehmer *et al.* in the 27-eV region. For energies above 20 eV, the present results remain a few percent higher than those of Kennerly *et al.*, although they have similar shape. A comparison of the e^+-SF_6 and e^--SF_6 total cross sections (Fig. 11) shows that the e^- Q_T's are higher than the e^+ Q_T's at all the energies of comparison, with there being an indication of a tendency toward merging of the e^+ and e^- Q_T curves at the higher energies.

There is not sufficient information on the elastic and inelastic differential cross sections for the $e^{+,-}$-SF_6 system to allow us to estimate the errors of the present Q_T results associated with the incomplete discrimination against small-angle scattering. Absolute elastic differential cross sections for e^--SF_6 in the angular range of 20°–135° is reported by Srivastava *et al.*,[39] but these measurements do not extend to smaller angles.

ACKNOWLEDGMENTS

We would like to thank Dr. A. Jain for providing us with his $e^{+,-}$-CH_4 calculation results prior to publication and D. Jerius and Darryl Dalton for their assistance in various aspects of this project. This work is supported by the National Science Foundation. One of us (M.S.D.) acknowledges the receipt of a Yarmouk University research grant.

[1](a) Ch. K. Kwan, Y.-F. Hsieh, W. E. Kauppila, Steven J. Smith, T. S. Stein, M. N. Uddin, and M. S. Dababneh, Phys. Rev. Lett. **52**, 1417 (1984); (b) T. S. Stein and W. E. Kauppila, in *Electron and Atomic Collisions,* edited by D. C. Lorents, W. E. Meyerhof, and J. R. Peterson (North-Holland, Amsterdam, 1986), p. 105.

[2]K. Takayanagi and M. Inokuti, J. Phys. Soc. Jpn. **23**, 1412 (1967).

[3]W. E. Kauppila, M. S. Dababneh, Y.-F. Hsieh, Ch.K. Kwan, T. S. Stein, and M. N. Uddin, in *Abstracts of Contributed Papers, Thirteenth International Conference on the Physics of Electronic and Atomic Collisions, Berlin, 1983,* edited by J. Eichler, W. Fritsch, I. V. Hertel, N. Stolterfoht, and U. Wille (North-Holland, Amsterdam, 1983), p. 303; Ch.K. Kwan, Y.-F. Hsieh, W. E. Kauppila, Steven J. Smith, and T. S. Stein, in *Abstracts of the XIV International Conference on the Physics of Electronic and Atomic Collisions, Palo Alto, CA, 1985,* edited by M. J. Coggiola, D. L. Huestis, and R. P. Saxon (Elsevier, New York, 1985), p. 332; Ch.K. Kwan, Y.-F. Hsieh, W. E. Kauppila, Steven J. Smith, T. S. Stein, M. N. Uddin, and M. S. Dababneh, in *Positron (Electron)-Gas Scattering,* edited by W. E. Kauppila, T. S. Stein, and J. M. Wadehra (World Scientific, Singapore, 1986), p. 241.

[4]W. E. Kauppila, T. S. Stein, J. H. Smart, M. S. Dababneh, Y. K. Ho, J. P. Downing, and V. Pol, Phys. Rev. A **24**, 725 (1981).

[5]W. E. Kauppila, T. S. Stein, G. Jesion, M. S. Dababneh, and V. Pol, Rev. Sci. Instrum. **48**, 822 (1977).

[6]P. G. Coleman, T. C. Griffith, G. R. Heyland and T. L. Killeen, *Atomic Physics* (Plenum, New York, 1975), Vol. 4, pp. 355–371.

[7]M. Charlton, T. C. Griffith, G. R. Heyland, and G. L. Wright, J. Phys. B **13**, L353 (1980).

[8]M. Charlton, T. C. Griffith, G. R. Heyland, and G. L. Wright, J. Phys. B **16**, 323 (1983).

[9]T. C. Griffith, M. Charlton, G. Clark, G. R. Heyland, and G. L. Wright, in *Positron Annihilation* (North-Holland, Amsterdam, 1982), pp. 61–70.

[10]E. Bruche, Ann. Phys. (Leipzig) **83**, 1065 (1927).

[11]G. Sunshine, B. B. Aubrey, and B. Bederson, Phys. Rev. **154**, 1 (1967).

[12]A. Salop and H. H. Nakano, Phys. Rev. A **2**, 127 (1970).

[13]T. W. Shyn and W. E. Sharp, Phys. Rev. A **26**, 1369 (1982).

[14]G. Dalba, P. Fornasini, R. Grisenti, G. Ranieri, and A. Zecca, J. Phys. B **13**, 4695 (1980).

[15]A. Zecca, R. S. Brusa, R. Grisenti, S. Oss, and C. Szmytkowski, J. Phys. B **19**, 3353 (1986).

[16]T. Wedde and T. G. Strand, J. Phys. B **9**, 1091 (1974).

[17]S. P. Khare and D. Raj, Indian J. Pure Appl. Phys. **20**, 528 (1982).

[18]J. P. Bromberg, J. Chem. Phys. **60**, 1717 (1974).

[19]K. Floeder, D. Fromme, W. Raith, A. Schwab, and G. Sinapius, J. Phys. B **18**, 3347 (1985).

[20]O. Sueoka and S. Mori, J. Phys. B **19**, 4035 (1986).

[21]A. Jain, Phys. Rev. A **35**, 4826 (1987).

[22]E. Barbarito, M. Basta, M. Calicchio, and G. Tessaro, J. Chem. Phys. **71**, 54 (1979).

[23]H. Tanaka, T. Okada, L. Boesten, T. Suzuki, Y. Yamamoto, and M. Kubo, J. Phys. B **15**, 3305 (1982).

[24]R. K. Jones, J. Chem. Phys. **82**, 5424 (1985).

[25]B. Lohman and S. J. Buckman, J. Phys. B **19**, 2565 (1986).

[26]A. Jain and D. G. Thompson, J. Phys. B **15**, L631 (1982).

[27]A. Jain, Phys. Rev. A **34**, 3707 (1986).

[28]C. Ramsauer and R. Kollath, Ann. Phys. (Leipzig) **4**, 91 (1930).

[29]L. Vuskovic and S. Trajmar, J. Chem. Phys. **78**, 4947 (1983).

[30]A. Jain, J. Chem. Phys. **78**, 6579 (1983).

[31]N. Abusalbi, R. A. Eades, T. Nam, D. Thirumalai, D. A. Dixon, D. G. Truhlar, and M. Dupuis, J. Chem. Phys. **78**, 1213 (1983).

[32]H. S. W. Massey, E. H. S. Burhop, and H. B. Gilbody, in *Electronic and Ionic Impact Phenomena* (Clarendon, Oxford, 1969), Vol. II, p. 713.

[33]W. E. Kauppila, T. S. Stein, and G. Jesion, Phys. Rev. Lett. **36**, 580 (1976).

[34]H. S. W. Massey, *Negative Ions,* 3rd ed. (Cambridge University Press, Cambridge, England, 1976), p. 368.

[35]R. E. Kennerly, R. A. Bonham, and M. McMillan, J. Chem. Phys. **70**, 4 (1979).

[36]K. Rohr, J. Phys. B **12**, L185 (1979).

[37]J. Ferch, W. Raith, and K. Schroder, J. Phys. B **15**, L178 (1982).

[38]J. L. Dehmer, J. Siegel, and D. Dill, J. Chem. Phys. **69**, 5203 (1978).

[39]S. K. Srivastava, D. Trajmar, A. Chutjian, and W. Williams, J. Chem. Phys. **64**, 2767 (1976).